

Iron and Nickel line properties in the X–ray reflecting region of the Circinus Galaxy

Silvano Molendi¹, Stefano Bianchi² and Giorgio Matt²

¹*IASF–CNR, Via Bassini 15, I–20133, Milano, Italy*

²*Dipartimento di Fisica, Università degli Studi “Roma Tre”, Via della Vasca Navale 84, I–00146 Roma, Italy*

31 October 2018

ABSTRACT

We discuss the iron and nickel properties in the nuclear X-ray reflecting region of the Circinus Galaxy, studied with *XMM–Newton*. The main results are: a) from the depth of the Fe $K\alpha$ edge, a value of $A_{\text{Fe}}=1.7$ in number with respect to the cosmic value (as for Anders & Grevesse 1989) is measured, if the (not directly visible) illuminating spectrum is assumed to be that measured by BeppoSAX. If the slope of the primary power law is left free to vary, a steeper spectrum and a lower iron abundance (about 1.2) are found. b) From the Ni to Fe $K\alpha$ lines flux ratio, a nickel-to-iron abundance ratio of 0.055–0.075 is found. c) The Fe $K\beta/K\alpha$ flux ratio is slightly lower than expected, possibly due to a mild ionization of iron (which however cannot be much more ionized than x). d) The presence of the Fe $K\alpha$ Compton Shoulder, already discovered by *Chandra*, is confirmed, its relative flux implying Compton–thick matter. This further supports the identification of the reflecting region with the absorber.

Key words: galaxies: active – X-rays: galaxies – Galaxies: individual: Circinus Galaxy

1 INTRODUCTION

The Circinus galaxy, at the distance of about 4 Mpc, is the closest and brightest among Compton-thick Seyfert 2 galaxies (see Matt 2002a and Matt et al. 2000 for reviews). Its nuclear 2–10 keV X–ray spectrum is dominated by reflection from a spatially unresolved region (which hereinafter we will call the ‘torus’, Antonucci 1993) with a size less than about 15 pc (Sambruna et al. 2001a). Most of the line spectrum (Sambruna et al. 2001b; Guainazzi et al. 1999; Matt et al. 1996) can be explained in terms of a single, mildly ionized reflector (Bianchi et al. 2001) even if a second, more ionized reflecting region is required to account for the faint He–like Fe $K\alpha$ line detected by the *Chandra/HETG* (Sambruna et al. 2001b). Given the brightness of the source and the dominance of the cold reflection component, the Circinus Galaxy is ideal to study the physical, chemical and geometrical properties of the torus.

Above 10 keV, the nuclear emission becomes visible, piercing through a cold absorber with $N_{\text{H}} = 4 \times 10^{24} \text{ cm}^{-2}$ (Matt et al. 1999). It is natural to identify the absorber with the reflector, as the latter should be Compton–thick, as implied by its spectrum (e.g. Matt et al. 2003) and by the relative flux of the Compton Shoulder (Bianchi et al. 2002; Matt 2002b; this paper), i.e. the part of the line profile due to photons which are scattered before escaping the matter. With this assumption, from the modeling of the line spec-

trum a value of about 0.2 pc for the inner radius of the torus can be derived (Bianchi et al. 2001).

In this Letter we analyze and discuss the hardest part of the spectrum with the aim of studying the iron and nickel properties, taking advantage of the unprecedented sensitivity of *XMM–Newton* at these energies. A complete spectral and spatial analysis is beyond the scope of this paper, and is deferred to a future work.

2 DATA REDUCTION

The Circinus Galaxy was observed by *XMM–Newton* for about 110 ks on August 6 and 7 2001. The EPIC p-n and MOS1 cameras were operated in full frame mode while the EPIC MOS2 was operated in large window mode. ODF files were downloaded from the public archive and processed using version 5.4.1 of the SAS software. Further screening for soft proton flares and residual hot pixels was performed using procedures described in Baldi et al. (2002). The effective exposure times after cleaning are 75, 77 and 70 ks for MOS1, MOS2 and p-n respectively. For our spectral analysis we used pattern 0 to 12 events for MOS1 and MOS2 while for p-n we accumulated separately single and double events spectra. Spectra for all three cameras were extracted from a 30'' radius circle centered on the source peak. Two nearby

arXiv:astro-ph/0305217v1 13 May 2003

sources lie within this radius, but were excluded by excising circles with a $7''$ radius centered on the respective peaks. Inspection of a 6–10 keV image shows that the intensity at the peak for these sources is less than a 10–15% of the Circinus peak intensity. Exclusion of their core is therefore sufficient to make contamination very small. Background spectra for the 3 cameras were extracted from annuli with bounding radii $90''$ and $150''$ centered on the source, after having verified that in these regions no detectable sources were present. Redistribution matrices and effective areas were generated using the RMFGEN and ARFGEN tools. Above ~ 2 keV the standard energy binning for matrices generated by RMFGEN is 50 eV for p-n and 5 eV for MOS. Because our aim is to perform detailed spectroscopy on Fe and Ni lines observed between 6 and 8 keV, we have chosen a finer binning of 1 eV for both MOS and p-n matrices. The effective areas were of course generated with the same binning. For the fitting procedure, we rebinned the data to have at least 20 counts per bin, in order to ensure applicability of χ^2 statistics.

3 DATA ANALYSIS AND RESULTS

In Fig. 1 the (p-n, single event) spectrum of the nucleus above 5 keV is shown. Three emission lines are obviously present, readily identified with iron $K\alpha$ and $K\beta$ as well as nickel $K\alpha$. The expected energies of these lines, assuming neutral atoms, are: 6.400 keV (actually a doublet, composed by a 6.391 keV and a 6.405 keV line); 7.058 keV (a doublet, with energies of 7.057 keV and 7.058 keV) and 7.472 keV (a doublet, with energies of 7.461 keV and 7.478 keV). All line energies are from Kaastra & Mewe (1993). For each doublet, the intensity ratio between the two lines is 1:2, and the given energies are the weighted mean.

In the following, unless explicitly stated, we will adopt the cosmic element abundances given by Anders & Grevesse (1989), which are 4.68×10^{-5} for iron and 1.78×10^{-6} for nickel (by number with respect to hydrogen); and the fluorescent yields given by Kaastra & Mewe (1993), which for neutral atoms are: 0.304 (iron $K\alpha$); 0.038 (iron $K\beta$); 0.368 (nickel $K\alpha$).

In the following, we will also assume that the absorbing material is dust-free. In fact, from the observed N_{H} of $4 \times 10^{24} \text{ cm}^{-2}$ a value of $A_{\text{V}}=2000$ is expected for a gas-to-dust ratio like that in the ISM of our own galaxy (Savage & Mathis 1979), while the derived value from IR observations is 50 only (Moorwood 1996).

We fitted separately the spectra from MOS1, MOS2, p-n single events and double events. The p-n single events gives values of the line energies close to the expected ones for neutral atoms (the other instruments giving values systematically higher, MOS1 being the most discrepant, giving e.g. 6.436 for the iron $K\alpha$). Therefore, in the following we will limit the analysis to this instrument which is the one with the larger signal-to-noise. In principle, as it is possible that the matter is mildly ionized, this choice is somewhat arbitrary, but it is supported by the $K\beta$ line flux, as explained in Sec. 3.3.

The spectrum in the 4.5 to 13 keV range has been fitted with a model composed of a cold reflection component (model PEXRAV in XSPEC), produced by a power-law with $\Gamma = 1.56$ and an exponential cutoff at $E_{\text{C}} = 56$ keV (Matt et

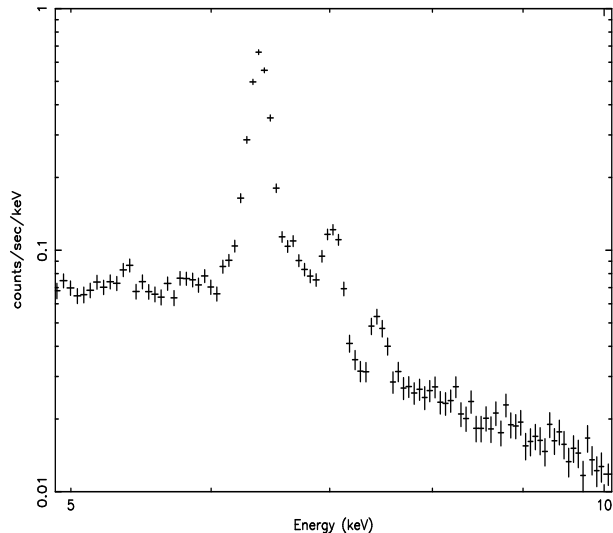


Figure 1. The 5–10 keV p-n spectrum.

al. 1999, Bianchi et al. 2001), and the three emission lines mentioned above, all of them described by a gaussian model with $\sigma=1$ eV (i.e. much less than the instrument energy resolution) and a redshift of 0.0015 (Freeman et al. 1997). The χ^2 is poor (381/117 d.o.f.), largely due to residuals around the iron $K\alpha$ line (see Fig. 2). Leaving the width of the line free to vary, the fit improves significantly ($\chi^2=206/116$ d.o.f.), but residuals are still visible, and the width of the line, $\sigma = 42$ eV, is not easy to explain if we assume that the line emitting matter is the molecular torus*. It seems more likely that the line ‘wings’ are instead due to the Compton shoulder (Bianchi et al. 2002), redwards of the line core, and to the He-like iron line (Sambruna et al. 2001b), bluewards of the line core. The Compton shoulder is indeed expected on theoretical ground (Matt 2002b), while the He-like iron line probably originates from reflecting circumnuclear ionized matter. We therefore added two more lines, with energies fixed at 6.3 keV (Matt 2002b) and 6.68 keV, respectively (the width of the line core, as well as that of the added lines, held fixed to 1 eV for simplicity). The fit improves significantly ($\chi^2=157/115$ d.o.f.), and no strong systematic residuals are left (Fig. 3). The significance of each line is $>99.99\%$, according to the F-test. The Compton shoulder is actually expected to have a finite width, but unfortunately its profile (Sunyaev & Churazov 1996, Matt 2002) is different from any XSPEC model. As a check, we tried for the Compton Shoulder also gaussians with $\sigma=40$ and 70 eV (the latter value corresponding to a FWHM of the same order of the total width of the Shoulder). A worse fit (χ^2 of 162/115 and 179/115, respectively) is obtained, but the fluxes of both the Shoulder and the line core remain almost unchanged.

The best fit results are summarized in Table 1. All errors refer to 90% confidence level for one interesting parameter. It is worth noting that the measured iron $K\alpha$ line energy

* If the line is emitted by a torus rotating around the black hole with keplerian velocity, and assuming a black hole mass of $1.7 \times 10^6 M_{\odot}$ (Greenhill et al. 2003) and an inner radius of the torus of 0.2 pc (Bianchi et al. 2001), the expected value of σ is about 2 eV.

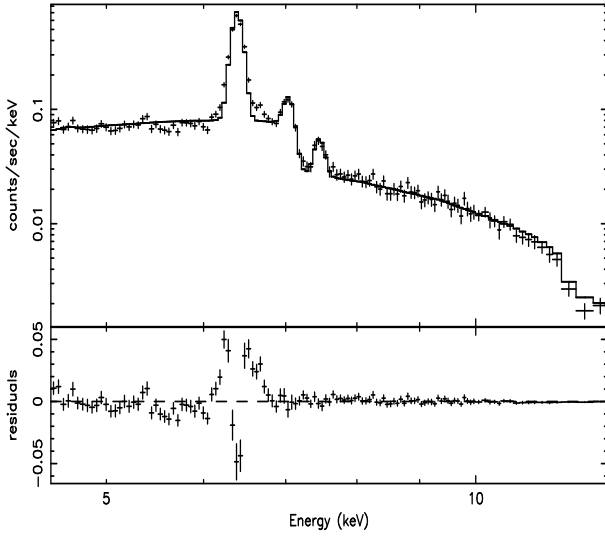


Figure 2. The best fit spectrum and residuals when fitted with a cold reflection component plus three narrow gaussian lines accounting for the iron $K\alpha$ and $K\beta$ lines, and the nickel $K\alpha$ line.

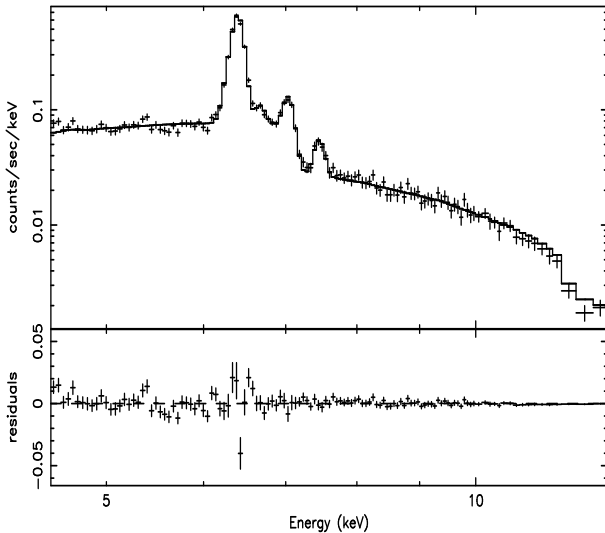


Figure 3. The best fit spectrum and residuals when the Compton Shoulder and the He-like iron $K\alpha$ line are included.

constrains, at the above confidence level, the ionization state of iron (before the photoionization) to be between XII and XIII (House 1969), or to be exactly XVII if the MOS1 value is considered. While of course, given the present uncertainties on the instruments calibrations, these results cannot be taken too literally, they highlight the potentially extraordinary precision of the measure. More solid constraints on the ionization states can be derived from the Fe $K\beta/K\alpha$ lines ratio, as discussed in Sec. 3.3.

3.1 The Fe abundance

The iron abundance is directly measured by the depth of the iron edge in the Compton reflection continuum, and it is measured with respect to the elements responsible for the photoabsorption below the edge, mainly oxygen and neon but with significant contributions from magnesium, silicon

[t]

Table 1. Best fit results

Γ	1.56 (fixed)
E_c [keV]	56 (fixed)
A_{Fe}^a	$1.72^{+0.14}_{-0.09}$
E (Fe $K\alpha$) [keV]	$6.413^{+0.002}_{-0.002}$
F (Fe $K\alpha$) [10^{-5} ph cm $^{-2}$ s $^{-1}$]	$21.4^{+0.6}_{-0.6}$
EW (Fe $K\alpha$) [eV]	1160
E (Fe $K\beta$) [keV]	$7.051^{+0.008}_{-0.009}$
F (Fe $K\beta$) [10^{-5} ph cm $^{-2}$ s $^{-1}$]	$2.94^{+0.23}_{-0.24}$
EW (Fe $K\beta$) [eV]	201
E (Ni $K\alpha$) [keV]	$7.466^{+0.013}_{-0.014}$
F (Ni $K\alpha$) [10^{-5} ph cm $^{-2}$ s $^{-1}$]	$1.49^{+0.18}_{-0.24}$
EW (Ni $K\alpha$) [eV]	175
F (Fe He-like $K\alpha$) [10^{-5} ph cm $^{-2}$ s $^{-1}$]	$1.36^{+0.25}_{-0.24}$
EW (Fe He-like $K\alpha$) [eV]	72
F (Fe $K\alpha$ CS) [10^{-5} ph cm $^{-2}$ s $^{-1}$]	$4.28^{+0.41}_{-0.55}$

^a in solar units (Anders & Grevesse 1989) by number.

and sulphur. The high quality of the spectrum permits to estimate this parameter with high (statistical) precision, i.e. less than 10%. The result, i.e. $A_{\text{Fe}} \sim 1.7$, has been obtained assuming an illuminating spectrum as that derived from the BeppoSAX observation (Matt et al. 1999). Leaving the photon index free to vary (and with the high energy exponential cut-off fixed at 100 keV), a significantly better fit is found ($\chi^2=138/114$ d.o.f., the improvement being significant at the 99.98% confidence level), and the iron abundance decreases to about 1.2, a value which is more consistent with the iron $K\alpha$ EW (e.g. Matt et al. 2003 and references therein). The best fit power law photon index is 1.90 ± 0.05 .

In all fits described so far the inclination angle of the reflector has been held fixed to the XSPEC default value of 63° . Leaving this parameter free to vary no significant difference in the value of A_{Fe} is found.

In conclusion, given the uncertainties on the primary continuum as well as on the geometry of the reflector (the PEXRAV model is for a plane-parallel slab), we can conclude that the iron abundance is confined to be between 1 and 2. This is in agreement with the results obtained by comparing the line EW and the Compton reflection continuum in a sample of Seyfert 1 galaxies (Perola et al. 2002).

3.2 The Ni abundance

In order to derive, from the observed Ni to Fe $K\alpha$ line fluxes, the relative abundances of the two elements, we calculated the expected values of their ratio, using the method proposed by Basko (1978) and valid for a semi-infinite plane-parallel slab that is isotropically illuminated. For the nickel line we included in the calculations both the unscattered and once scattered line photons, while for the iron line, for which the two components are separated in the fit procedure, we included only photons in the line core. The values of the calculated ratio range from 0.03 to 0.045, depending on the inclination angle and the assumed power law index. The measured value, 0.07 with an error of less than 20%, is significantly larger, strongly indicating a nickel-to-iron overabundance. In the calculations, we adopted cosmic abundances. However, the results do not depend much on the iron and nickel abundances, provided that they vary together. In fact, if e.g. both iron and nickel are twice the cosmic value, we calculate that the flux of the nickel line increases only by a factor ~ 1.3 (because of the increased photoelectric absorption), similar to the increase expected for the flux of the iron line (Matt et al. 1997), so leaving the need for a nickel-to-iron overabundance unchanged.

It must also be noted that, as we fitted the Ni line with a narrow gaussian, part of its Compton Shoulder could be lost in the fitting procedure, so possibly further increasing the relative Ni overabundance.

Finally, we recall that in the calculations we have used the Anders & Grevesse (1989) abundances. If we instead use the Anders & Ebihara (1982) set, which differs mainly in having the iron abundance 1.4 times lower, the expected values are of course not much different from what we measure. The same is true if we use the Grevesse & Sauval (1998) or, even more, the Holweger (2001) sets. Put it in a different way, our results implies that the nickel-to-iron absolute abundance ratio is around 0.055-0.075, independently of course of the set of solar abundances chosen for reference.

3.3 The Fe $K\beta/K\alpha$ ratio

The ratio between the Fe $K\beta$ and $K\alpha$ (core only) lines is 0.14 with a statistical error of about 10%. This number slightly increases, but within the statistical error, when the power law index of the illuminating continuum is kept free. The expected value, again using the Basko (1978) formulae, is 0.155-0.16 (depending on the inclination angle), only marginally consistent with the measured value. Again, it is possible that in the fit procedure part at least of the Fe $K\beta$ Compton Shoulder is lost, so reducing the discrepancy. Alternatively, it is possible that the actual value of the $K\beta/K\alpha$ probabilities is slightly lower (for instance, Kikoin (1976) quoted a ratio of 17:150), or that the iron is moderately ionized; interestingly, the observed value is the one expected from Fe IX or X (Kaastra & Mewe 1993), close to what found from the p-n single event iron $K\alpha$ line energy. Instead, a too small value is expected for more ionized atoms, and of course no $K\beta$ line at all is expected for Fe XVII (the ionization state found from the MOS1) or more, when M electrons are no longer present.

3.4 The Compton Shoulder

The ratio between the iron $K\alpha$ Compton Shoulder and the line core is $20\pm 3\%$, fully consistent with the value found by *Chandra* (Bianchi et al. 2002). The greater precision of the present estimate with respect to the *Chandra* one strengthens the case for a Compton-thick reflector (Matt 2002b), giving further support to the identification of the reflector with the absorber. It is important to note that, while absorption provides information on the optical depth of the line-of-sight material, features in reflection, being integrated over the whole visible part of the matter, give information on the average value of the optical depth. The very fact that the amount of Compton shoulder is consistent with the optical depth derived from absorption suggests that the material is fairly homogeneous, so supporting the classical toroidal model for the cold circumnuclear matter[†].

4 SUMMARY

The results discussed in this paper may be summarized as follows:

a) From the Fe $K\alpha$ edge a value of $A_{\text{Fe}}=1.7$ in number with respect to solar (using the set of values given by Anders & Grevesse 1989) has been found, assuming the primary illuminating continuum measured by BeppoSAX (Matt et al. 1999). If the slope of the primary power law is left free to vary, a steeper spectrum and a lower iron abundance (about 1.2) is found.

b) From the flux ratio of the Ni to Fe $K\alpha$ lines, a nickel-to-iron abundance ratio of 0.055-0.075 is found, i.e. a factor of 1.5-2 Ni relative overabundance compared to the Anders & Grevesse (1989) cosmic values, and instead roughly consistent with the Anders & Ebihara (1982) set. To the best of our knowledge this is the first unambiguous X-ray detection of a Ni line in an AGN. Previous detections, like in the ASCA spectrum of Ark 564 (Turner et al. 2001) and in the BeppoSAX spectrum of Circinus itself (Guainazzi et al. 1999) were affected by confusion with the Fe $K\beta$ line.

c) The Fe $K\beta/K\alpha$ flux ratio is ~ 0.14 , somewhat lower than expected. A possible explanation is that the iron is mildly ionized, but not much more than Fe X, otherwise the Fe $K\beta$ line emission would be much fainter than observed (and of course absent at all for Fe XVII or more).

d) The presence of the Fe $K\alpha$ Compton Shoulder, already discovered by Bianchi et al. (2002) in the *Chandra*/HETG spectrum, is confirmed. The relative flux of the Compton Shoulder is $20\pm 3\%$, fully consistent with the *Chandra* finding, and implying Compton-thick matter (Matt 2002b). This provides further support to the identification of the reflecting region with the absorber and suggests that the torus is fairly homogeneous.

[†] See Matt & Guainazzi 2003 for a case in which the optical depth derived from the Compton Shoulder is an order of magnitude lower than that of the intervening matter.

ACKNOWLEDGMENTS

GM and SB acknowledges ASI and MIUR (under grant COFIN-00-02-36) for financial support.

REFERENCES

- Anders E., Grevesse N., 1989, *Geo. Cosm. Acta* 53, 197
Anders E., Ebihara M., 1982, *Geo. Cosm. Acta* 46, 2363
Antonucci R., 1993, *ARA&A* 31, 473
Baldi A., et al., 2002, *ApJ*, 564, 190
Basko M.M., 1978, *ApJ*, 223, 268
Bearden J.A., 1967, *Rev. Mod. Phys.*, 39/1, 78
Bianchi S., Matt G., Iwasawa K., 2001, *MNRAS*, 322, 669
Bianchi S., et al., 2002, *A&A*, 396, 793
Freeman K.C., et al., 1977, *A&A*, 55, 445
Greenhill L.J., et al., 2003, *ApJ*, in press (astro-ph/0302533)
Grevesse N., Sauval A.J., 1998, *Space Sci. Rev.*, 85, 161
Guainazzi M., et al., 1999, *MNRAS*, 310, 10
Holweger H., 2001, Joint SOHO/ACE workshop "Solar and Galactic Composition". Edited by Robert F. Wimmer-Schweingruber. AIP Conference proceedings vol. 598, p.23
Kaastra J.S., Mewe R., 1993, *A&AS*, 97, 443
Kikoin I.K., 1976, *Tables of Physical Quantities*, Atomizdat, Moscow
Matt G., et al., 1996, *MNRAS*, 281, L69
Matt G., Fabian A.C., Reynolds C.S., 1997, *MNRAS*, 289, 175
Matt G., et al., 1999, *A&A*, 341, L39
Matt G., et al., 2000, *MNRAS*, 318, 173
Matt G., 2002a, *Phil. Trans. Royal Society A*, 360, 2045
Matt G., 2002b, *MNRAS*, 337, 147
Matt G., Guainazzi M., 2003, *MNRAS*, in press (astro-ph/0303626)
Matt G., Guainazzi M., Maiolino R., 2003, *MNRAS*, in press (astro-ph/0302328)
Moorwood A.F.M., 1996, *A&A*, 315, L109
Perola G.C., et al., 2002, *A&A*, 389, 802
Sambruna R., et al., 2001a, *ApJ*, 546, L9
Sambruna R., et al., 2001b, *ApJ*, 546, L13
Savage B.D., Mathis J.S., 1979, *ARA&A*, 17, 73
Sunyaev R.A., Churazov E.M., 1996, *Ast. Letters*, 22, 648
Turner T.J., et al., 2001, *ApJ*, 561, 131